J Mater Sci (2006) 41:7562–7570
DOI 10.1007/s10853-006-0841-x

Nano and micro structural studies of thin films of ZnO

Harish Bahadur · S. B. Samanta · A. K. Srivastava · K. N. Sood · R. Kishore · R. K. Sharma · A. Basu · Rashmi · M. Kar · Prem Pal · Vivekanand Bhatt · Sudhir Chandra

Received: 28 October 2005 / Accepted: 18 November 2005 / Published online: 12 October 2006

Abstract Zinc oxide thin films grown by sol–gel and RF sputtering methods have been characterized. The characterization techniques used involve ellipsometry, optical absorption, scanning tunneling microscopy, scanning and transmission electron microscopy. The films grown by sol–gel spin method which followed zinc acetate route exhibited a smoother texture than the films, which were deposited by using zinc nitrate route. The later type of films showed a dendritic character. Nano-structured fine grains of size ranging from 20 to 60 nm were observed with zinc nitrate precursor film. Individual grains show a sharp contrast with different facets and boundaries. Crystal planes and lattice parameters calculated by electron diffraction and X-ray diffraction are quite close and in agreement with the reported values in literature. Scanning tunneling microscopy has been used for measuring the average roughness of the surface and estimating the lattice constants. The STM studies of RF sputtered films, although showing a ZnO structure, exhibited a disturbed lattice. This was presumably due to the fact that after deposition the films were not annealed. Nanographs of 2D and 3D view of atomic positions of ZnO have been presented by using scanning tunneling microscopy.

H. Bahadur (✉) · S. B. Samanta · A. K. Srivastava · K. N. Sood · R. Kishore · R. K. Sharma · A. Basu · Rashmi · M. Kar
National Physical Laboratory, Dr. K.S. Krishnan Road, New Delhi 110012, India
e-mail: hbahadur@yahoo.com

P. Pal · V. Bhatt · S. Chandra
Centre for Applied Research in Electronics, Indian Institute of Technology Delhi, Hauz-Khas, New Delhi 110016, India

Introduction

Thin films of zinc oxide have varied technological applications such as piezoelectric transducer [1], transparent conductor [2], surface acoustic wave devices [3, 4] and a variety of sensors [5, 6]. Consequently, thin films of ZnO are grown by a variety of methods such as vacuum evaporation [7], sputtering [8], MOCVD [2, 9], sol–gel [10] chemical solution deposition [11], chemical vapor deposition [12] and spray pyrolysis [13] etc. It is known that ZnO has a wurtzite structure having a number of alternating planes composed of fourfold coordinated O^{2-} and Zn^{2+} ions stacked alternatively along c-axis of hexagonal unit cell with lattice constants; $a_0 = 0.3255$ nm and $c_0 = 0.5216$ nm. The tetrahedral coordination in ZnO results in non-central symmetric structure and the consequent piezoelectric and pyroelectric nature of the material. It can thus be considered as two interpenetrating hexagonal closed-packed lattices of Zn and O.

The preparation and characterization of ZnO thin films has been the subject of continuous research for a long time because the properties of ZnO films depend upon the method of preparation. Currently, there is a great interest in the methods of creating nanostructures

on surfaces by various self-organizing techniques [14]. These nanostructures form the basis of nanotechnology applications in sensors and molecular electronics. The nanostructures exhibit novel electrical, mechanical, chemical and optical properties, which are believed to be due to the surface confinement effects of nanostructures in one dimension (1D). These 1D objects are of great importance in understanding some basic physics related phenomena in the low dimension systems to form the basis of next generation high performance nano-devices.

In this work, we present our results on thin films of ZnO grown by sol–gel spin methods as well as RF sputtering. Two types of sols were prepared using zinc nitrate and zinc acetate as precursor materials. RF sputtering was carried out by using a stoichoimetric target of ZnO. The characterization techniques involved optical absorption, ellipsometry, scanning electron microscopy with energy dispersive analysis, X-ray diffraction, transmission and scanning tunneling microscopy. The results presented provide the information about the structural characteristics of the films. However, many results exhibit that all the films grown are not of high quality but the studies carried out do show some important and new information about the manner in which the growth kinetics of the film is governed and proceeds both in sol–gel spin as well as RF sputtering methods. The information revealed from such characterization techniques become important to decide the quality of the film before its incorporation in the device for MEMS based sensor applications, which is an important part of project. A proper characterization of the film would not only give reliability of a sensor but obviously reduce the associated cost of fabrication of such sensors.

Preparation of thin films

Sol–gel spin method

The films were grown by sol–gel technique on silicon and fused quartz substrates. The growth procedure consisted of first making the surface of the silicon substrate hydrophilic by boiling the wafer in 70% HNO_3 followed by rinsing in de-ionized water and subsequent drying. This process oxidizes the Si surface to SiOH and improves its adhesion. The sol was prepared by two different routes. The first route involved dissolving 10 gm of zinc nitrate $[Zn(NO_3)_2 \cdot 6H_2O]$ in ethylene glycol monomethyl ether $[CH_3O–CH_2–CH_2OH]$ to form the zinc solution. The other route of sol preparation was to prepare 10% solution of zinc acetate $[Zn(CH_3COO)_2 \cdot 2H_2O]$ by dissolving 10 gm of zinc acetate in 100 ml of boiling isopropyl alcohol at 84 °C. This was followed by clarifying the turbid solution by adding a few drops of diethanolamine. For the film preparation, a Si wafer was mounted on a spinner and the sol was placed on top of it and the wafer was allowed to spin at the rate of 3000–4000 rpm. This step was followed by drying the coated wafer at 100 °C and subsequent baking at 450 °C for 1 h. Films were prepared using both the routes one by one. Multiple coatings were done to obtain the workable thickness of the film using both the routes of sol preparation. The ellipsometric data show that for ten coatings, the film thickness was only of the order of 20–25 Å.

RF sputtering method

The zinc oxide films were deposited in an RF (13.56 MHz) diode sputtering unit (Alcatel, France). The pumping system consists of a standard rotary pump, diffusion pump and a liquid nitrogen trap. A 3-inch diameter stoichoimetric target of ZnO was used. Sputtering was carried out in pure argon atmosphere in 'sputtered-up' configuration. The Si wafers of 2-inch diameter were clamped on to the substrate holder. The sputtering process was performed in the pressure range of 5–20 mTorr and the RF power ranging from 100 to 300 W. Films were deposited at various sputtering pressures and RF power. The target to substrate distance was kept constant at 45 mm for all the depositions. No external substrate heating was done during the deposition. However, during sputtering process the temperature due to self-heating is expected to rise to approximately 150 °C.

Results and discussion

Optical and X-ray measurements

Optical absorption data on the deposited films was measured using Shimadzu UV3101 PC spectrophotometer. For measurements in the UV and optical region, the films were coated onto a substrate of amorphous quartz. Figure 1 depicts the representative optical absorption of the films using zinc nitrate precursor. In both the cases, the absorption band was located around 372 nm giving characteristic absorption of ZnO. The band gap calculated from the absorption data has been found to be approximately 3.3 eV.

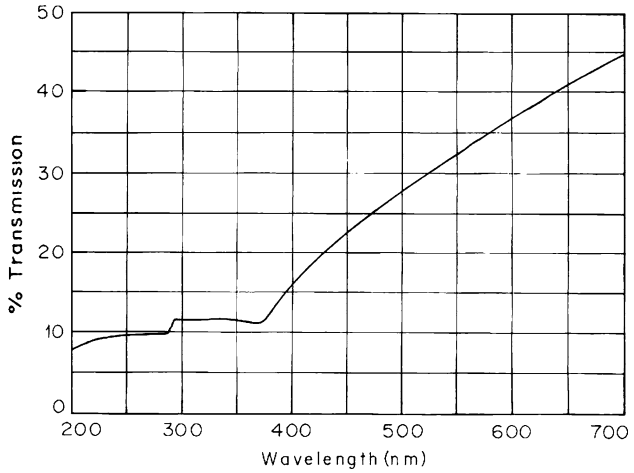

Fig. 1 A representative optical absorption spectrum of ZnO for a film thickness in the range of 80–90 nm grown by sol–gel spin method using zinc nitrate as precursor material

X-ray diffraction measurements were carried out on a Bruker AXS D8 Advance diffractometer using Diffrac^{plus} software. Diffractograms were recorded in grazing incidence geometry. The incidence angle was fixed at 1.5° and 2θ was scanned in the required range. The radiation used was CuKα. The diffracted beam had a long soller slit and a LiF monochromator. That the films were crystalline in nature has been shown in the XRD pattern of Fig. 2 for the film, which was prepared using zinc nitrate as the precursor material. Several prominent crystal planes have been resolved clearly. However, the XRD pattern shows that there is no preferential orientation of crystal planes for the film sample.

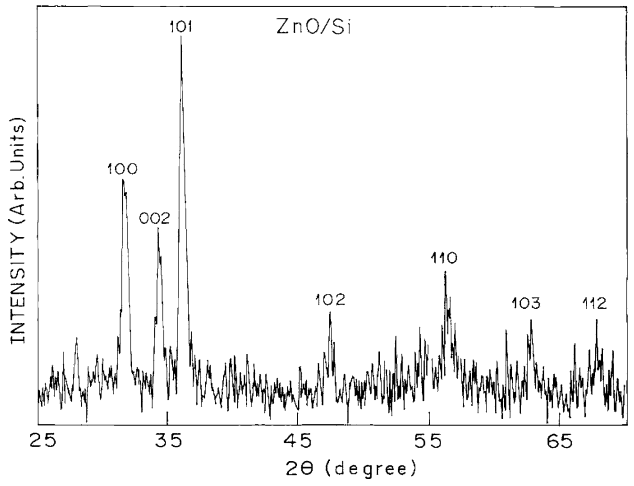

Fig. 2 XRD pattern of ZnO film on a silicon substrate grown by sol–gel spin method using zinc nitrate as precursor material

Ellipsometric measurements

Ellipsometric measurements were made on a Rudolph Research manual null-type ellipsometer, at a single wavelength of 546.1 nm, using angles of incidence in the range 50–75 degrees. Measurements were made at three angles of incidence and the best, most consistent results for refractive index (n), extinction coefficient (k) and thickness (d) of the thin film sample were calculated using in-house developed software. Calculations of n, k, and d were done using in-house developed software. Using the measured values of the ellipsometric angles Ψ and Δ at each of the three different angles of incidence, and searching in specified range of values for n and k, the value of d is calculated for each pair (n,k) and a common value (or small range of values) for d for all three angles of incidence is searched for. Once such a value (or small range of values) for d is found. This d and the corresponding (n,k) values are taken as solution for (n,k,d) of the film. Table 1 shows the results for different film samples using zinc nitrate and zinc acetate precursors on both quartz and silicon substrates. It may be mentioned here that the ellipsometric measurements on the film grown on silicon wafer by using zinc acetate precursor could not be performed with our manual single wavelength ellipsometer, due to the fact that film was highly absorbing and nonuniform. Table 2 presents the ellipsometric data for the films grown by RF sputtering method. The data show that the film is quite uniform throughout.

From the tables, it may be noticed that the refractive index and extinction coefficient values are different in different films. This shows that different films have varying compactness. The sol–gel spin grown film would be more compact than the film grown by RF sputtering. This would be due to the fact that in the sol–gel process, the precursor molecules are uniformly dispersed and thus under normal temperature conditions arrange themselves more closely than in the RF sputtering process where the growth is done on the molecule to molecule basis. In the case of sol–gel grown films, sintering would further increase the compactness. This increase of compactness will be due to reduction in the volume in proceeding from zinc salt to ZnO. Sintering would also lead to reducing the voids, which would be an additional contributory factor in increasing the compactness. On the other hand, no sintering is involved in the RF sputtering process. The film is deposited on the basis of molecule by molecule. This therefore gives the possibility of a large number of voids. Table 2 shows that the RF sputtered film has a higher value of refractive index in the central region

Table 1 Ellipsometric data of n, k and d for the thin films of ZnO grown by sol–gel spin method

Precursor	Substrate	Refractive index (n)	Extinction coeff. (k)	Film thickness (d)
$[Zn(NO_3)_2 \cdot 6H_2O]$	Silicon wafer	1.83 ± 0.03	0.47 ± 0.02	227 ± 15 nm
$[Zn(CH_3COO)_2 \cdot 2H_2O]$	Silicon wafer	.....	.....	.....
$[Zn(NO_3)_2 \cdot 6H_2O]$	Fused quartz	1.63 ± 0.02	0.085 ± 0.005	200 ± 2 nm
$[Zn(CH_3COO)_2 \cdot 2H_2O]$	Fused quartz	1.64 ± 0.01	0.16 ± 0.03	275 ± 15 nm

than at the edges. This would be due to the fact that during sputtering most of the sputtered atoms, as a natural course, follow the straight path to the central part of the substrate and therefore stick to the central region of the wafer substrate and, depending upon the variation of the electric field gradient, a lesser number is likely to go to the edges go the edges. Thus, the central region of the film becomes more compact than the edges. This view point also supports the fact that the film thickness is more in the central region than the edges as can be seen from the Table 2. It is expected that the central portion of the film will have lesser voids than in the edges. Our future investigations will resolve this issue.

Scanning tunneling microscopy

In the present work, we have used the Scanning tunneling microscopy (STM) to look for the atomic arrangement of a surface. A commercial model Nano Scope II from Digital Instruments Inc, Santa Barbara, CA was used for investigating the surfaces of the grown films. We have obtained the atomic-image scale image of the ZnO film material. This is done by sensing the corrugations in the electron density on the surface. These corrugations arise from the positions of the atoms on the surface. The instrument was operated at ambient temperature using Pt-Ir nanotip. The real space grey scale images were obtained in the constant current mode with the negative bias voltage of the order of 500 mV. Three-dimensional profiles of the different locations of the surface were generated to observe surface roughness, surface defects and in determining the size and conformation of molecules and aggregates on the surface.

Table 2 Ellipsometric data of n, k and d for ZnO film deposited by the RF sputtering method

Surface location of the film	Refractive index (n)	Extinction coeff. (k)	Film thickness (d)
Central region	1.760 ± 0.010	0.003 ± 0.001	214 ± 2 nm
Near the edge	1.710 ± 0.010	0.004 ± 0.002	212 ± 1 nm

Figure 3 depicts a representative surface topographical feature of the film grown by using zinc acetate precursor. A 3D view of the surface corresponding to the same surface location is shown in Fig. 4. The results show that the film has an average roughness of 0.45 nm and the standard deviation of 0.07. A 2D lattice of the film is shown in Fig. 5 and its magnified 3D version in Fig. 6. Figures 7 and 8 show the nanographs for the film grown by RF sputtering at two different surface locations. The overall lattice structure in this case is not

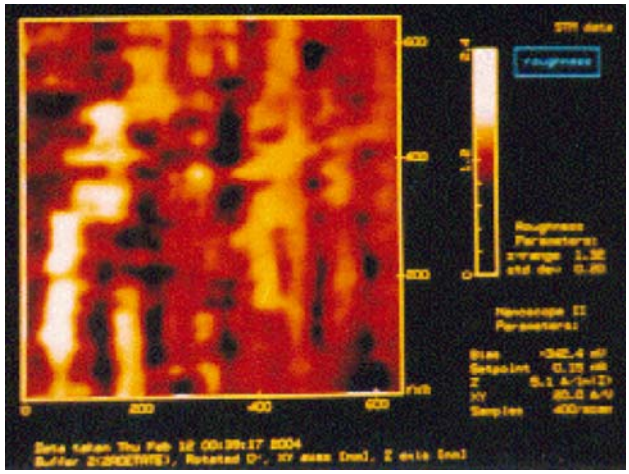

Fig. 3 Scanning tunneling micrograph of a ZnO film grown by sol–gel process showing the surface undulations

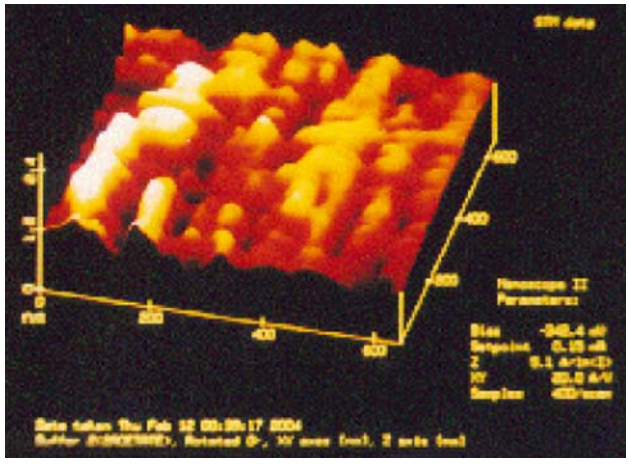

Fig. 4 A 3D view of the film shown in Fig. 3

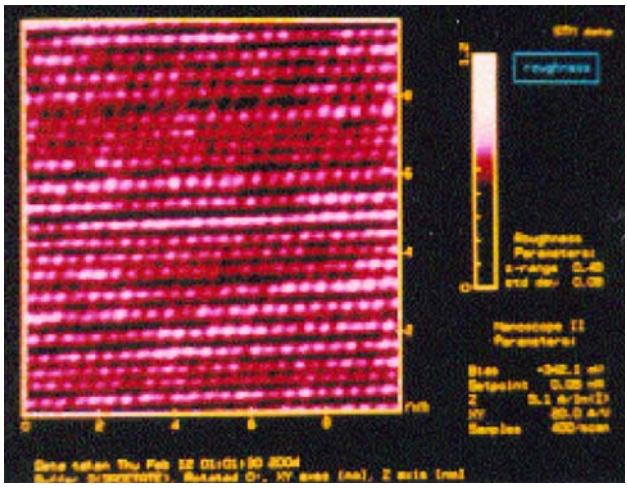

Fig. 5 Scanning tunneling micrograph of a ZnO film grown by sol–gel process showing its lattice structure in 2D

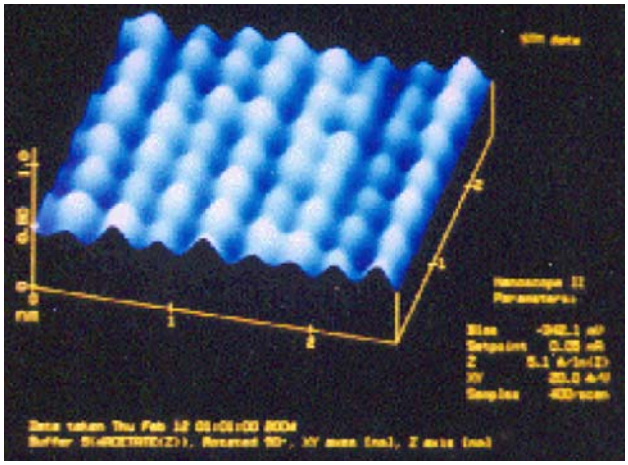

Fig. 6 A magnified 3D view of the film shown in Fig. 5

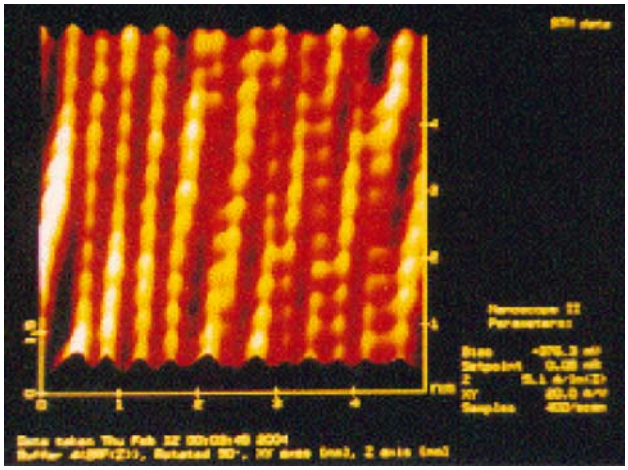

Fig. 7 STM micrograph of a RF sputtered ZnO film showing its showing its distorted lattice structure in 2D

as uniform as shown by the films grown by sol–gel spin method. It was noticed to exhibit a distorted lattice. Perhaps this would be due to the fact that after the deposition, the films were not thermally annealed. A 3D view of Fig. 8 is shown in Fig. 9. For the sol–gel grown films, the measurements were done to estimate the lattice constants a_0 and c_0 as shown in Figs. 10 and 11 respectively. The measured values are $a_0 = 0.3255(\pm 0.0004)$ nm and $c_0 = 0.529(\pm 0.0008)$ nm respectively. These values are in agreement with the reported values of unit cell parameters of ZnO in literature.

From the STM pictures, it can be observed that the surface morphology of the films prepared by two different techniques changes with the method of preparation. The films grown by sol–gel spin method (Figs. 5, 6) show a much uniform morphology than that of the RF sputtered films shown in Figs. 7 and 8. In

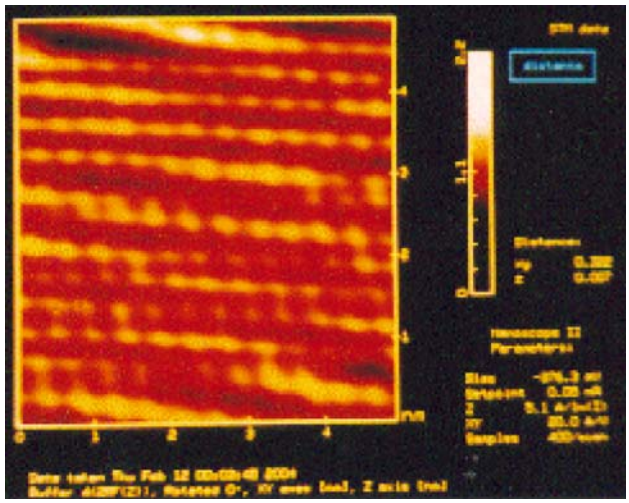

Fig. 8 STM micrograph of the same RF sputtered film of ZnO as shown in Fig. 7 but at a different surface location of the film in 2D

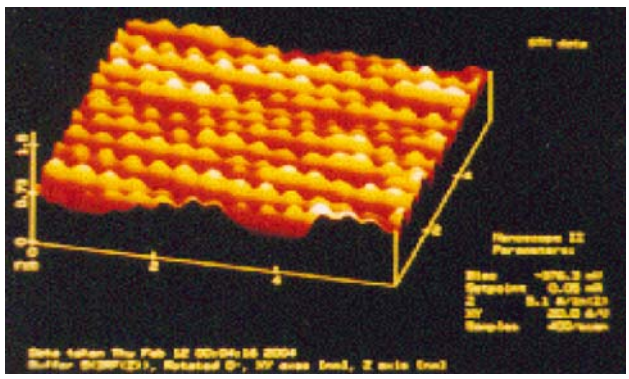

Fig. 9 A 3D view of Fig. 8 showing the lattice distortions

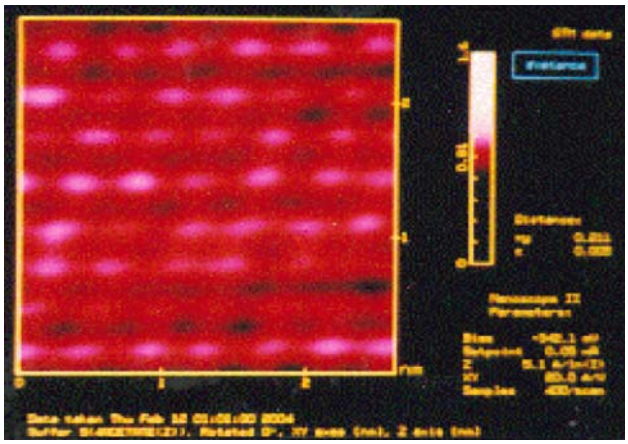

Fig. 10 STM micrograph of the sol–gel grown ZnO film measuring the lattice constant a_0 of ZnO. The film was prepared by using zinc acetate as the precursor material

case of sol–gel spin method, the film is expected to be more compact and uniform than the film grown by the RF sputtering. The precursor molecules in the sol are believed to be uniformly dispersed and thus arrange themselves more closely than in the RF sputtering process where the growth is done on the molecule to molecule basis. In the case of sol–gel process, sintering further increases the uniformity and compactness of the film. The films grown by RF sputtering process were not annealed and thus showed a distorted lattice as observed by the scanning tunneling spectroscopy.

Electron microscopic studies

Micro-structural analysis of the sol–gel grown ZnO films on Si substrates were carried out both by scanning electron microscope (SEM model LEO-0440) and the transmission electron microscope (TEM model JEOL TEM 200Cx). The SEM was equipped with ISIS 300 Oxford microanalysis system (EDS attachment). It must be mentioned here that the reason for using both SEM and TEM was that while the SEM provides the morphology of the surface, the TEM gives the grain size and shapes at higher magnification within that morphology. The specimens in the SEM were mounted on a 15 mm diameter stub and a thin layer of gold was sputtered onto it. The stubs were then fixed on the viewing stage of the SEM equipped with *xyz* movement as well as rotational and tilt facilities. The specimen was scanned thoroughly at a lower magnification in order to see the uniformity of the film.

The SEM examination revealed that the films prepared by zinc nitrate precursor showed a polycrystalline structure having dendrite growth with agglomeration of dendrites in some areas as shown in Fig. 12. On the other hand, the film grown by using zinc acetate precursor shows uniform structure with needle shaped particles distributed throughout the area scanned such as shown in Fig. 13. The needles have their length between 0.2 and 0.8 μm. A comparison of these micrographs suggest that the films prepared by using zinc nitrate show a rapid and random crystallization compared to that using zinc acetate. The EDS analysis (Fig. 14) of one of these films, prepared by using zinc acetate as the precursor material, revealed the presence of zinc, silicon, nitrogen and oxygen. The traces of nitrogen could broadly be attributed to the fact that diethanolamine was used in the sol preparation. The films thus consisted mainly of ZnO.

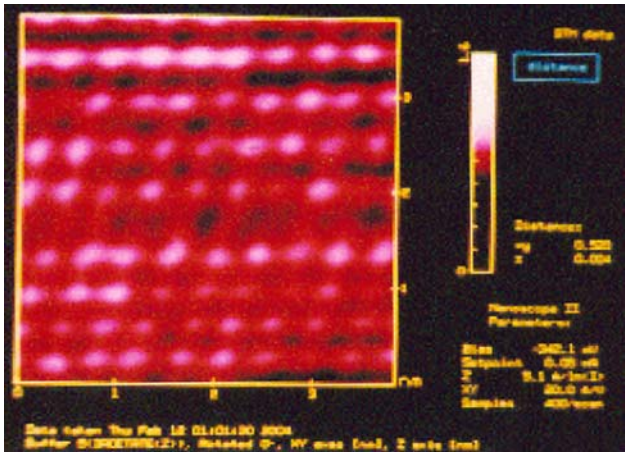

Fig. 11 STM micrograph of the sol–gel grown ZnO film measuring the lattice constant c_0 of ZnO. The film was prepared by using zinc acetate as the precursor material

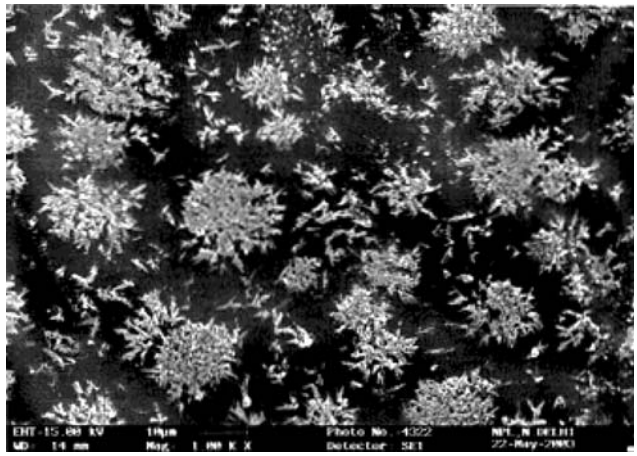

Fig. 12 SEM topograph of a ZnO film prepared by using zinc nitrate as precursor material. The topographic features exhibit dendrites on the surface

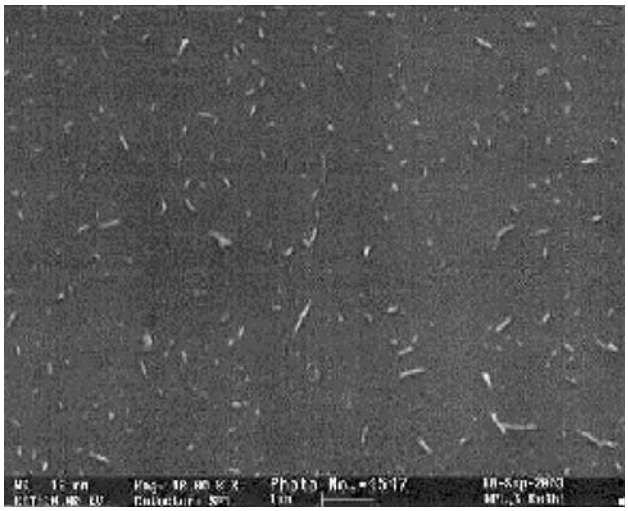

Fig. 13 SEM topograph of ZnO film prepared by using zinc acetate as precursor material. The topographic features exhibit needle type structure in the size range from 0.2 to 0.8 μm

The TEM specimens were prepared in the following routine way. First, the film was removed from the substrate by using a sharp surgical blade. In this process, a few mm^2 area of the film was available for investigation in good order without any physical or mechanical damage to the film. This part of the film was then floated on acetone. Further, it was lifted on a 200 mesh perforated Cu-grid of 3.05 mm diameter. Subsequently, the Cu grid was transferred in the TEM holder to observe the film under the microscope.

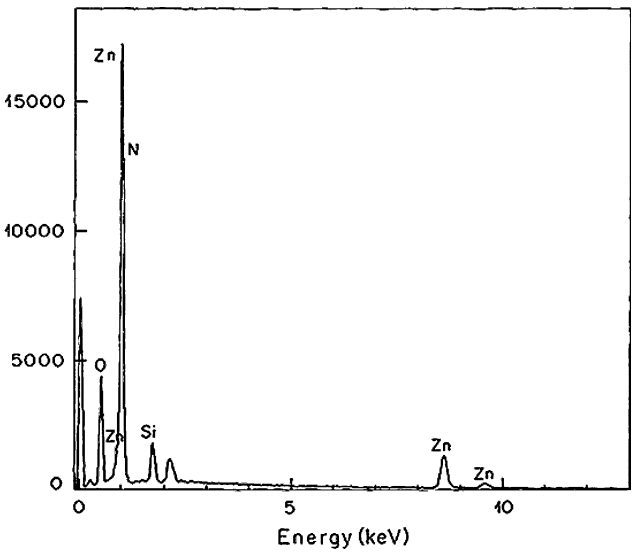

Fig. 14 EDS spectrum of a sol–gel grown ZnO film using zinc acetate as the precursor material. The traces of nitrogen could broadly be attributed to the fact that diethanolamine was used in the film preparation

At high magnification, transmission electron microscopy (TEM JEOL TEM Cx), operated at 200 kV, was carried out to investigate the different morphologies observed under SEM. These investigations of the films revealed many interesting features. Nano-structured fine grains with the size of about 20–60 nm with clear surface boundaries were observed within the needle shaped morphologies as seen in SEM. These micrographs are shown in Fig. 15 for the film grown on fused quartz substrate using zinc nitrate precursor. The individual grains show a distinguished contrast on the surface. In some cases, different facets with sharp edges may also be seen. A non-spherical shape and faceted morphology of these grains may be attributed to their crystallographic symmetry of the wurtzite ZnO and a preferred growth direction during deposition. It shows that the film is polycrystalline in nature with a random distribution of nano-grained ZnO in it. However, the absence of certain important reflections of hexagonal ZnO in the electron diffraction pattern elucidates that the film has certain texture with preferred growth direction.

TEM bright-field micrographs were recorded for the film using zinc acetate precursor as well. The microstructural investigations (Fig. 16) revealed that the structure of these films consists of fine dendrites with ultra-fine nanograins. The microstructural evidence has exhibited certain difference between the films prepared by zinc nitrate and zinc acetate precursors. It appears that in the zinc nitrate case, the grains with faceted morphology (Fig. 16) are formed whereas in the case of zinc acetate, the ultra-fine dendrites constitute the microstructure of film.

The microstructural observations as evidenced by high magnification studies under transmission electron microscope have clearly shown that the films processed

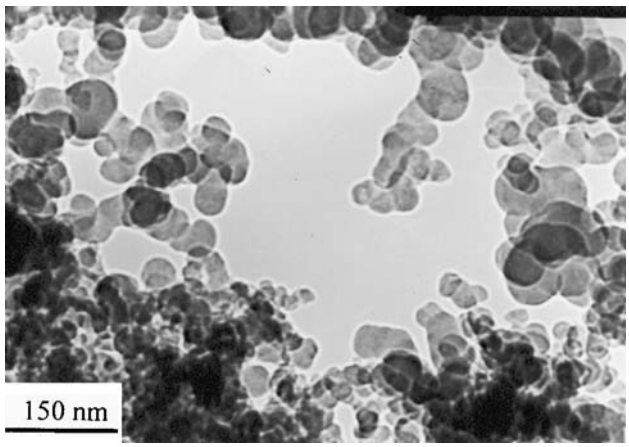

Fig. 15 TEM bright micrographs of ZnO film prepared by sol–gel spin method using zinc nitrate as precursor material

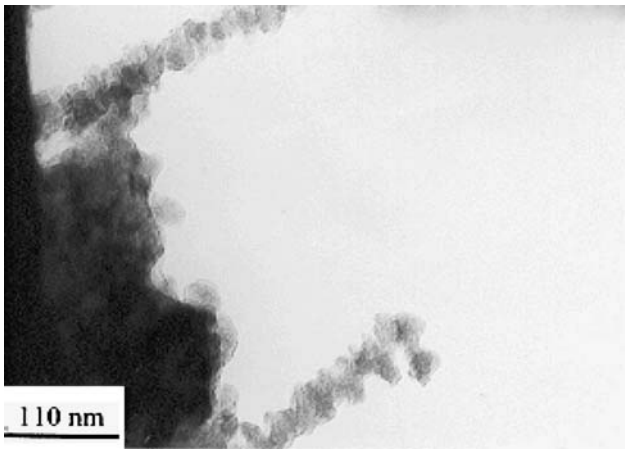

Fig. 16 TEM bright micrographs of ZnO film prepared by using zinc acetate as precursor material

by sol–gel techniques are nanostructured with fairly uniform grain-size distribution. It is known that nanograins have a significant amount of grain boundaries, which alter the properties of the material. This is because of change in scattering characteristics of energy/charge carriers at grain boundaries in comparison to the within the grains. Looking at the microstructure (Figs. 15, 16), it appears that the grain boundaries are forming a continuous distribution of dense network in the matrix and are curly in shape. Such structure of grain boundaries dominates the microstructure.

A selected area electron diffraction (SAED) pattern was recorded under TEM in proper recording conditions such as beam divergence and proper exposure time. Several regions were examined before the expose of SAED pattern. In all the areas, only limited rings were observed. SAED pattern for on one of films is shown in Fig. 17 for which the XRD has been depicted

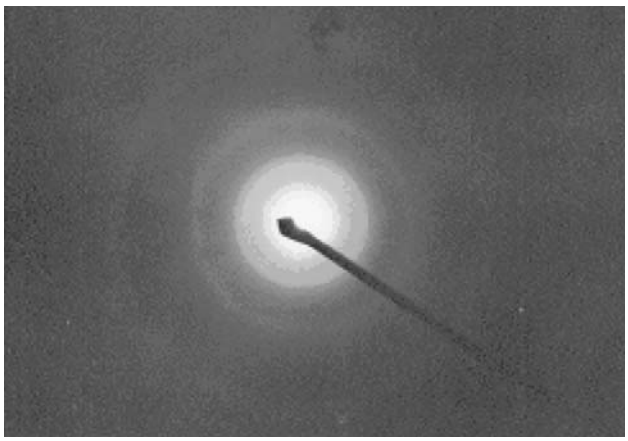

Fig. 17 Selected area electron micrograph of the ZnO film of Fig. 15 showing the crystalline nature of the film

in Fig. 2. The diffused contrast over the Debye ring would presumably be due to the combined effect of several grain boundaries present, in particular, nano sized ZnO grains on thin films. Since the SAED is the information about the orientation of crystallographic planes in a selected area of the film, it would be appropriate to visualize that these are local area textured films, as observed under TEM. The electron diffraction pattern of Fig. 17, however, clearly demonstrates three important planes of hexagonal structure (100, 101, 202) in the form of continuous rings in the reciprocal space with inter planar spacing of 0.28, 0.25 and 0.12 nm respectively. The electron diffraction studies thus reveal that the local areas of these microstructures have preferred growth, which textures the film. Since the grains are in the scale of nanometers, these rings appeared diffused in the electron diffraction pattern. It may be noticed from the XRD and SAD patterns that not all the planes as observed in the XRD spectrum (Fig. 2) are observable in the selected area electron diffraction (Fig. 17). This is understandable because normally XRD is a representative of the entire area of the film while the electron diffraction in from the selected area of the grain.

Summary and conclusion

ZnO thin films grown by sol–gel spin process and RF sputtering has been studied for their optical absorption, ellipsometry, XRD, SEM, EDS, TEM and STM. Results of all the characterization techniques have shown that primarily the films consisted of ZnO. Work in this direction is continued towards growing well oriented films for use in MEMS based sensors. However, the present investigations carried out on ZnO films grown by sol–gel and RF sputtering have shown the following broad results.

1. The films grown by zinc acetate and zinc nitrate as precursor materials show different morphological features. Films grown by zinc nitrate show rapid and random crystallization than the films grown by zinc acetate. A smoother topography is obtained for the films grown by using zinc acetate than for the films grown by zinc nitrate.
2. The films grown by RF sputtering have shown a lower refractive index than the films grown by sol–gel spin method. The lower refractive index of such films shows that these films are less compact than those grown by sol–gel spin method in the present investigation.

3. Scanning tunneling microscopy has revealed that the films grown by zinc acetate as precursor has more uniform lattice than the RF sputtered films in the present investigation.
4. Nano-structured ZnO grains of size ranging from 20 to 60 nm were obtained on the film grown by sol–gel spin process using zinc nitrate as precursor material. Individual grains have shown a sharp contrast with different facets and boundaries.

Acknowledgements This is a joint work between the National Physical Laboratory, New Delhi and the Indian Institute of Technology Delhi. The authors thank Dr. Vikram Kumar, Director of the National Physical Laboratory for his interest, encouragement and support in this work.

References

1. Yamazaki O, Mitsuyu T, Wasa K (1989) IEEE Trans Sonics Ultrasonics SU-27:369
2. Hu J, Gordon G (1992) J Appl Phys 71:880
3. Hickernell FS (1980) IEEE Trans Sonics Ultrasonics SU-32:621
4. Gupta V, Mansingh A (1996) J Appl Phys 80(2):1063
5. Arya SPS, Srivastava ON (1988) Cryst Res Technol 23:669
6. Tai W-P, Oh J-H (2002) J Mater Sci: Mater Electron 13:391
7. Ma J, Ji F, Ma H-L, Li S-Y (1995) J Vacuum Sci Tech A13:92
8. Minani T, Nanto H, Takata S (1985) Jpn J Appl Phys 24(8):L605
9. Kim JS, Marzouk HA, Reucroft PJ, Hamrin CM (1992) Thin Solid Films 217:133
10. Ohyama M, Kouzuka H, Yoko T (1997) Thin Solid Films 306:78
11. Saeed T, O'Brien Paul (1995) Thin Solid Films 271:35
12. Mar LG, Timbrell PY, Lamb RN (1993) ibid 223:341
13. Olvera M de la L, Maldonado A (2003) Phys Stat Sol (a) 196:410
14. Wang ZL (2004) J Phys Condens Matter 16:R829–R858. Institute of Phys Publishing